http://dx.doi.org/10.5012/bkcs.2013.34.1.35

Articles

Metabolic Rebalancing of CR6 Interaction Factor 1-Deficient Mouse Embryonic Fibroblasts; A Mass Spectrometry-Based Metabolic Analysis

Surendar Tadi,[†,‡] Soung Jung Kim,[†] Min Jeong Ryu,[†] Taeseong Park,[§] Ji-Seon Jeong,[‡] Young Hwan Kim,[§] Gi Ryang Kweon,[#] Minho Shong,[†] and Yong-Hyeon Yim[‡,*]

[†]*Research Center for Endocrine and Metabolic Diseases, Chungnam National University School of Medicine, Daejeon 301-721, Korea*
[‡]*Korea research Institute of standards and Science, Daejeon 305-340, Korea. [*]E-mail: yhyim@kriss.re.kr*
[§]*Korea Basic Science Institute, Cheongwon-gun 363-883, Korea*
[#]*Department of Biochemistry, Chungnam national University School of Medicine, Daejeon 301-721, Korea*
Received August 13, 2012, Accepted October 4, 2012

Metabolic analysis of CR6 interacting factor 1 (*Crif1*) deficient mouse embryonic fibroblasts with impaired oxidative phosphorylation has been carried out using LC-MS/MS and GC-MS methods. Metabolic profiles of the *Crif1* deficient cells were comprehensively obtained for the first time. Loss of oxidative phosphorylation functions in mitochondria resulted in cancer-like metabolic reprogramming with consumption of majority of glucose carbon from up-regulated glycolysis to produce lactate, suppressed utilization of glucose carbon in the TCA cycle, increased amounts of amino acids. The changes in metabolic profile of the *Crif1* deficient cells are most probably a consequence of metabolic reprogramming to meet the needs of energy balance and anabolic precursors in compensation for the loss of major oxidative phosphorylation functions.

Key Words : CRIF1, Metabolic analysis, Mass spectrometry

Introduction

CR6 interacting factor 1 (CRIF1) has been originally discovered as nuclear protein playing a role of cell cycle regulator, growth regulator and transcriptional cofactor.[1-5] CRIF1's co-presence both in the nucleus and mitochondria, however, raised the possibility of its additional role in mitochondria. Recent research finally characterized its mitochondrial function as a new mitoribosome-associated factor playing a critical role in the integration of oxidative phosphorylation (OXPHOS) complexes into the inner-mitochondrial membrane.[6] Loss of CRIF1 results in significant defects and deficiencies in OXPHOS complexes and functions, especially for complex I, III, IV and V, which are key elements for the production of major energy molecules. Hence, marked changes and rebalancing in energy metabolism and other related metabolism can be expected in *Crif1*-deficiency. For example, release of increased amount of lactate in culture media, where *Crif1*-knockout cells were grown, was observed.[6] Reduced expression of CRIF1 was observed for some cancers and its potential role in carcinogenesis was also discussed.[1] Taken together, metabolic readjustment similar to cancer may be expected in *Crif1*-deficiency.

Metabolomic analysis of *Crif1* knockout cells is anticipated to provide more comprehensive understanding of the altered regulation and adaptation of metabolism for *Crif1*-deficiency. Metabolomics has been widely used to obtain the comprehensive metabolic fingerprint of diverse biological system.[7] Mass spectrometry-based metabolome analysis, especially, made it possible to obtain metabolomic data sets with ever increasing size and reliability by the advances of high performance mass spectrometry and highly efficient computational tools.[8] It also allows in-depth understanding of complicated metabolic networks and controls in a biological system. Many research groups have conducted studies on metabolomics with various mass spectrometry platforms. Especially, recent researches on cancer metabolism elucidated detailed metabolic adjustments for survival and proliferation. Investigation on the metabolic profiles of colon and stomach cancer showed metabolic adaptation represented as enhanced glycolysis with high lactate production, accumulation of amino acids and anaplerotic utilization of glutamine to satisfy increasing demands for biosynthesis.[9] Metabolic flux profiles of melanoma cell lines were also investigated with stable isotope tracking analysis using [U-^{13}C] glucose and [U-^{13}C] glutamine.[10] In the metabolic flux analysis, relative fluxes of metabolites through individual metabolic reactions and pathways can be evaluated by monitoring the degrees of ^{13}C-labeling for individual metabolites along relevant metabolic pathways with the consideration of number of carbons transferred in each metabolic reactions. For example, the use of [U-^{13}C] glucose in the flux analysis allows the investigation of metabolic flux through

glycolysis and pentose phosphate, and TCA cycle pathways. On the other hands, the use of [U-^{13}C] glutamine is very useful to obtain the information on the metabolic flux related with anabolic glumaminolysis and gluconeogenesis. In addition to the Warburg effect[11] well-known in cancer cells, substantial contribution of glutamine to the tricitric acid (TCA) cycle and fatty acid synthesis was demonstrated in the melanoma cells. Metabolic flux analysis using [U-^{13}C] glutamine also provided evidence of reverse (reductive) TCA cycle flux for glutamine utilization.

In the present study, a metabolic profiling of *Crif1* knock-out mitochondrial embryonic fibroblasts (MEFs) has been carried out and compared with that of normal MEFs. To find out the changes in metabolism, we measured all key metabolites of glycolysis, TCA cycle and amino acid pathways. Static up- and down-regulations of glycolytic and TCA cycle metabolites were observed using LC-MS/MS and further supported by metabolic flux information obtained by stable isotope tracking analysis using [U-^{13}C] glucose based cell culture and high resolution LC-MS method. Amino acid metabolites were analyzed by GC-MS with derivatization. Metabolic analysis presented here unveiled, for the first time, the metabolic reprogramming of *Crif1* deficient cells to compensate for the loss of OXPHOS.

Experimental

Chemicals and Reagents. Dulbecco's Modified Eagle Medium (DMEM) and phosphate buffer were purchased from Invitrogen (Carlsbad, CA, USA). [U-^{13}C] glucose was obtained from Cambridge Isotope Laboratories, Inc. (Andover, MA, USA). All standards for glycolysis and TCA cycle metabolites, amino acid standards, ammonium acetate, tributylamine, hepatofluro butyric acid, 1-butanol, hydrochloric acid and methanol were purchased from Sigma-Aldrich (St. Louise, MO, USA). Br-AMP and D4-alanine, which were used as internal standards, were also purchased from Sigma-Aldrich.

Isolation of Embryonic Fibroblasts, Immortalization, MSCV Infection, and Transfection. Wild type and *Crif1* deficient MEFs were prepared as previously.[12] In brief, embryonic fibroblasts were isolated from E13.5 after treatment of trypsin/EDTA. Isolated primary MEF cells were immortalized by transfection with SV40-large T antigen. For murine stem cell virus (MSCV) infection, a high-titre virus soup was produced with gp2-293 cells transfected with the pMSCV (Clontech) and VSV-G vectors. Embryonic fibroblasts were infected for 24 h, and the infected cells were selected with removal of uninfected cells. Subsequent transient transfections of primary and immortalized MEFs were performed with Lipofectamine PLUS (Invitrogen) and a Microporator (Digital Biotechnology, South Korea). Immunoprecipitation and electrophoretic mobility shift assay was performed according to the manufacturer's instructions.

Cell Culture, Isotope Labeling and Sample Collection. Isolated wild type and *Crif1* deficient MEFs were grown in DMEM with 10% fetal bovine serum (GIBCO) substituted with 1% penicillin streptomycin (GIBCO) and maintained at 37 °C with 5% CO_2 supply. To check the influence of ROS in MEFs, wild type and *Crif1* deficient MEFs cells were treated with 1 mM of NAC for 24 h which is known as ROS scavenger previously.[13] Culture plates were maintained for 48 h as before. Cells were washed with phosphate buffer, crunched with ice cold 80% methanol and harvested into separate vials.[14]

Quantification of Total Protein. Total protein concentration in the cells was determined with Bradford reagent (Sigma-Aldrich). The assay was performed according to manufacturer's protocol in 96 well plates. In brief, 5 μL of cell lysate was added to micro well plate, 250 μL of Bradford reagent was added, shaken for a while and incubated in dark at room temperature for 40 min. UV absorbance was measured at 595 nm with BIO-RAD micro plate reader (n = 5). Protein concentration was determined by comparing the UV absorbance against Bovine serum albumin standard curve.

Western Blot Analysis. Cultured cells were washed with ice-cold PBS, maintained on ice for 10 min and re-suspended in isotonic homogenization buffer (250 mM sucrose, 10 mM KCl, 1.5 mM $MgCl_2$, 1 mM Na-EDTA, 1 mM Na-EGTA, 1 mM dithiothreitol, 0.1 mM phenylmethylsulfonyl-fluoride, 10 mM Tris-HCl (pH 7.4) along with proteinase inhibitor cocktail (Roche). Re-suspended cells were homogenized with Dounce homogenizer; Homogenate was centrifuged at 30 × g for 5 min to remove unbroken cells. From the supernatant nuclei and heavy mitochondria fractions were fractionated at 80 × g for 10 min and 6,000 × g for 20 min, respectively. After spinning down the mitochondrial fraction, the supernatant was further subjected to centrifugation at 20,000 × g for 20 min, and the final supernatant was used as the cytosolic fraction. The nuclear fraction was washed three times with homogenization buffer containing 0.01% NP-40. Western blot analysis was performed with standard method as stated elsewhere antibodies were obtained from: anti-CRIF1 (SantaCruz, sc-134882), Tom40 (Santa Cruz, sc-11414), α-Tubulin (Sigma-Aldrich, T5168).

Oxygen Consumption Rate and Glucose Uptake Measurement. Oxygen consumption rate (OCR) in mitochondria was measured using a Seahorse XF-24 extracellular flux analyzer (Seahorse Bioscience). Sensor cartridge was placed in calibration buffer supplied by Seahorse Bioscience a day before and incubated at 37° in non CO_2 atmosphere. Cells were cultured in Seahorse XF-24 plates till they attain the density of 20,000 per each well. Cultured cells were washed and incubated with assay medium (DMEM without bicarbonate) Temperature was maintained at 37 °C in the absence of CO_2. All reagents including media were optimized to pH 7.4 before assay. Three readings for OCR were taken before the injection and after the injection of each mitochondrial inhibitor. Following are the mitochondrial inhibitors used; oligomycin (2 μg/mL), CCCP (10 μM), and rotenone (1 μM). OCR was calculated with Seahorse XF-24 software provided with the instrument. After OCR measurements the same cell sample was used to measure the protein

concentration to ensure the cell number. Percentage was calculated by dividing change in the readings with average baseline readings. Glucose uptakes from normal and *Crif1* knockout cells were measured using 2-NBDG (fluorescent glucose analog) fluorescence assay kit (Invitrogen) following the protocol provided with the product.

Extraction and Quantification of Metabolites by LC-MS/MS. Cell pellet was extracted with 80% methanol as published before.[14] In detail, cell pellet was transferred into eppendorf tube and 50 μM of Br-AMP was added as an internal standard. The cell suspension was extraction with 300 μL of 80% methanol (n = 4), and supernatant was collected in a separate tube. The combined supernatant was filtered with 3 kDa molecular weight cutoff filter (Millipore), freeze-dried and reconstituted with 100 mM ammonium acetate prior to LC-MS/MS analysis. Reconstituted samples were subjected to LC-MS/MS as previously reported.[15] A gradient of eluent A (10 mM tributylamine, pH adjusted to 4.95 with acetic acid) and eluent B (methanol) at a flow rate of 0.2 mL/min was used to separate metabolites with Synergi Hydro-RP column (150 mm × 2.1 mm I.D., 4 μm 80 particles, Phenomenex, Torrance, CA, USA). Eluent B was 0%, initially, then, increased to 90% in 10 min and maintained 90% for 5 min. The LC eluents were introduced to LTQ linear ion trap mass spectrometer (Thermo Scientific, San Jose, CA, USA) equipped with electrospray ionization (ESI) interface. For reliable quantification of metabolites, selective reaction monitoring (SRM) mode was applied. LC-MS/MS results were normalized with internal standard and protein concentration. The quantification result was obtained after normalization with the internal standard and the total protein content.

GC-MS Sample Preparation and Analysis. For quantification of fatty acids, cells were cultured as stated above, harvested with ice cold methanol into screw capped glass tubes. Fatty acid methyl esters were prepared as described before.[16] One μg of pentadecanoic acid (C_{15}:0) was added as an internal standard. 1.5 mL of methanol and 0.3 mL of 8% hydrochloric acid was added for esterification derivatization. Cell suspension was incubated at 45 °C overnight. After cooling down to room temperature, 1 mL of hexane and 1 mL of H_2O were added, vortexed briefly and centrifuged in low speed. Fatty acid methyl esters were collected from upper hexane layer. Extraction step was repeated twice; combined extract was dried in a SpeedVac (Thermo scientific) and reconstituted in hexane. Methyl esters in hexane layer were analyzed using an Agilent HP6890 GC interfaced with an HP5973N MSD (mass selective detector). Fatty acid methyl esters were analyzed using the previous method.[17] Splitless injection of two microliters of sample was used. For GC separation DB-5 column was used. GC oven temperature was 150 °C initially and ramped up to 200 °C in 20 min, held for 2 min thereafter increased to 280 °C in 52 min. The full MS scans over *m/z* range of 60 to 800 were obtained and the peaks of the characteristic ion chromatogram for each fatty acid methyl esters were used for quantification. They were also normalized with the internal standard.

^{13}C-Labeled Metabolites Analysis. Metabolic labeling was performed using glucose-free DMEM medium supplemented with [U-^{13}C] glucose.[18,19] Rest of the cell culture conditions were the same as the non-labeling cell culture. Cells were harvested after 48 h of culture in the labeling medium. Chromatographic separation was performed on ACQUITY UPLC® system (Water, USA) using Acquity UPLC® Bridged Ethyl Hybrid column (BEH C18, 1.7 μm, 2.1 × 150 mm).[19] Column temperature was maintained at 65 °C. Mobile phase A was aqueous eluent with 1 mM ammonium acetate and 0.1% formic acid. Mobile phase B was 5:2 mixture of acetonitrile and isopropanol with 1 mM ammonium acetate, 0.1% formic acid. Flow rate was 200 μL/min. Gradient condition was 99% of eluent A initially, decrease to 50% of A at 1 min, 15% of A at 4 min, down to 0% of A at 5 min and then equilibrated for 1 min with 99% of eluent A again. UPLC separated metabolites were analyzed using Synapt G2S high resolution mass spectrometer equipped with ESI interface (Waters, USA). Data were collected in full scan mode in the range of *m/z* 50 to 1000. Data were processed with Masslynx software provided with instrument.

Amino Acid Analysis. The method for analysis of amino acid metabolites was as described previously.[20] MEFs were collected in an eppendorf tube. D_4-alanine was added as an internal standard just before extraction. Cells were extracted for amino acids with 300 μL of 20% methanol. Extraction was repeated twice and supernatants were collected in separate tubes. The extracts were dried in a SpeedVac and reconstituted in 200 μL of 3 M hydrogen chloride in 1-butonol and incubated in a temperature-controlled shaker for 15 min at 60 °C. Samples were cooled down to room temperature, reconstituted in 8:2 mixture of water and methanol with 0.1% formic acid. Amino acid metabolites were separated with Phenomenex Luna C18 column (5 μm, 2.0 × 150 mm). Gradient elution of water and methanol was used with addition of HFBA as an ion pairing agent. The LC eluents were introduced to LTQ linear ion trap mass spectrometer (Thermo Scientific, San Jose, CA, USA) equipped with ESI interface. All amino acids were monitored using the SRM mode and peak area was normalized with the internal standard and the protein concentration.

Results and Discussion

Characterization of *Crif1* Deficient Cells. CRIF1 is a CR6/gadd45-interacting factor associated with inner mitochondrial membrane.[2] Disruption of *crif1* gene results in impaired mitochondrial function due to defective integration of OXPHOS complexes into the inner mitochondrial membrane.[6] Oxidative phosphorylation in mitochondria is the major energy producing metabolism in non-proliferating cells, which is dependent on the efficient production of ATP utilizing pyruvate supplied by glycolysis through the tricarboxylic acid (TCA) cycle. Defective OXPHOS complexes, therefore, are expected to significantly influence the overall energy metabolism including the oxidative phosphorylation-

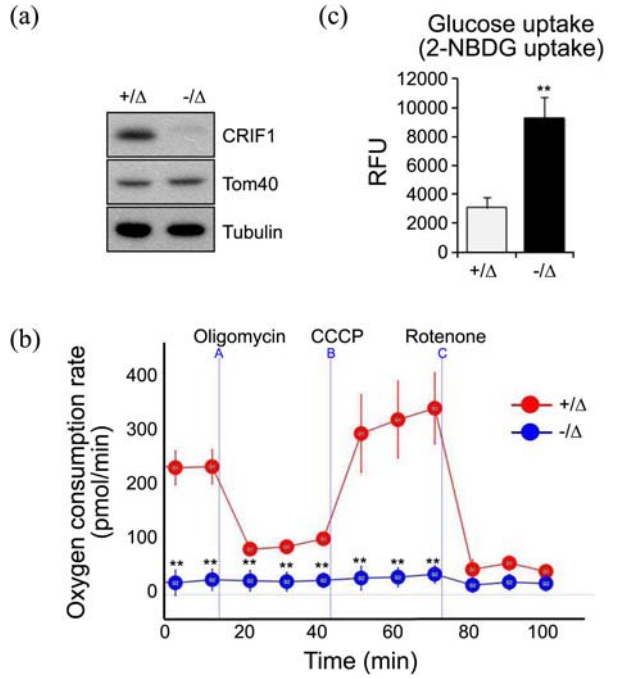

Figure 1. Effect of retrovirus mediated *Crif1* gene knockout; (a) Western blot analysis of whole cell lysates of MEFs with (–/Δ) and without (+/Δ) *Crif1* knockout, (b) evaluation of oxygen consumption rate using Seahorse XF-24 flux analyzer and provided protocol (n = 4, error bars indicate SD, **represent $p < 0.01$), (c) glucose uptake assay result for MEFs with (–/Δ) and without (+/Δ) *Crif1* knockout (n = 4, error bars indicate SD, **represent $p < 0.01$).

dependent production of ATP. To investigate the role of CRIF1 in the metabolic regulation, *Crif1* knockout MEFs were generated and confirmed with western blot analysis. As shown in Figure 1(a), CRIF1 was clearly identified in wild-type but not in knockout MEFs. The properties of the mutant cells were further confirmed by comparing their oxygen consumption rates (OCRs) and glucose uptake with those of wild-type cells. Due to the loss of OXPHOS subunits, OCRs of *Crif1*-deficient cells were lower than those of wild-type cells and irresponsive to the treatment of chemical inhibitors of mitochondrial respiratory chains as shown in Figure 1(b).[6] *Crif1* deficient cells are also known to show higher glucose consumption. Three fold increase of glucose uptake was observed for *Crif1* knockout cells, which was 9000 ± 2000 in relative florescence units, while it was 3000 ± 1000 for normal cells (Figure 1(c)). The lack of CRIF1 expression and inherent properties of *Crif1* knockout cells clearly demonstrates that *Crif1* deficient MEFs were prepared as designed previously.[6]

Glycolysis and Citric Acid Cycle Metabolites. *Crif1* knockout cells are known to produce increased amount of lactate with more consumption of glucose in the culture medium, which implicates enhanced glycolysis.[6] However, the detailed metabolic consequence of *Crif1* knock out has not been investigated yet. We analyzed several key metabolites in the glycolysis and TCA cycle pathways for *crif1* knock out cells and compared them with those for wild type cells using LC-MS/MS.

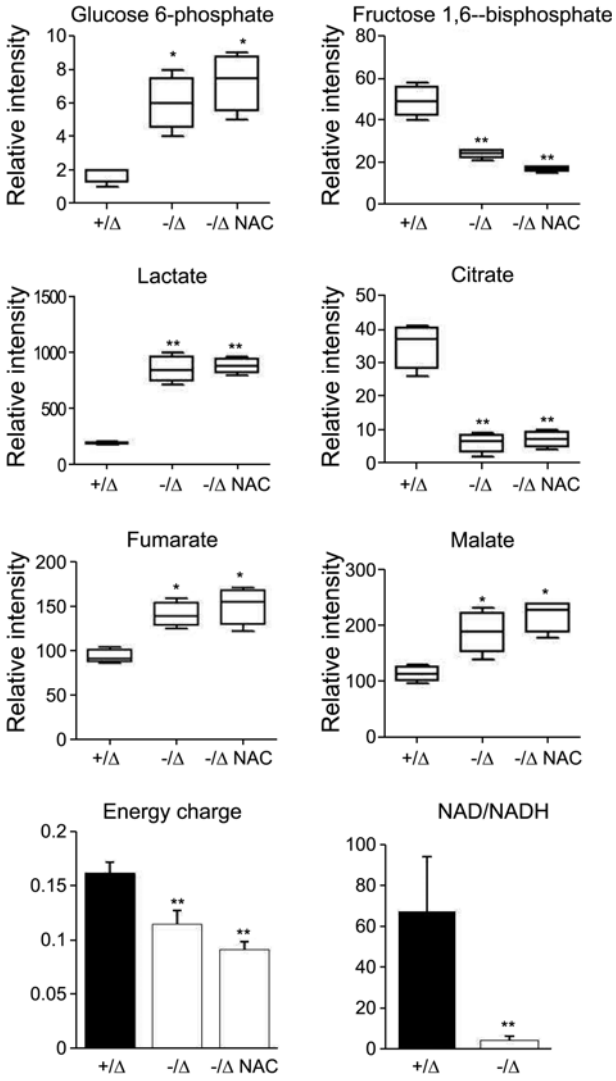

Figure 2. Relative abundances of static glycolysis and TCA cycle metabolites and energy molecules for normal (+/Δ), *Crif1* knockout MEF cells with (–/Δ NAC) and without (–/Δ) ROS scavenger, NAC, treatment (n = 4, error bars indicate SD, **$p < 0.01$, *$p < 0.05$).

Increased glucose consumption in *Crif1* knockout cells resulted in the increased level of glucose 6-phosphate (G6P) as shown in Figure 2. Because the phosphofructokinase 1 (PFK-1) is the rate-limiting enzyme in the glycolytic pathway,[21] which converts fructose 6-phosphate (F6P) to fructose 1,6-bisphosphate (FBP), the major glucose influx is expected to experience metabolic traffic jam here and accumulated more in the form of G6P and F6P in *Crif1* knockout cells. As observed previously,[6] the major glycolytic metabolic flux appeared to leak into lactate with about four-fold increase in its level in *Crif1* knockout cells. Decreased FBP level also reflects stronger metabolic outflux, mostly into lactate, after PFK-1. Lower pH due to accumulation of lactate in *Crif1* knockout cells allosterically inhibits the PFK-1 activity, but it seems to be more or less balanced with counter-effects of lower citrate and ATP levels. The ATP level is typically correlated with the energy

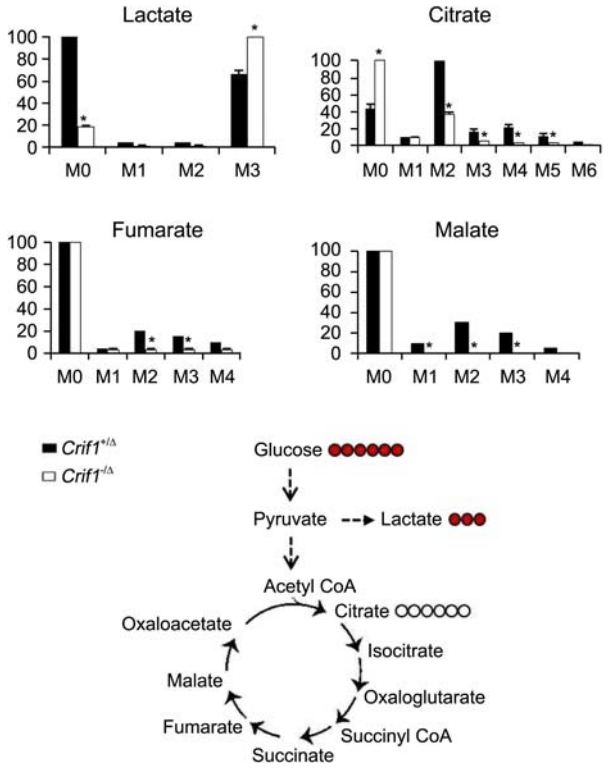

Figure 3. The metabolic flux analysis for normal (*Crif1*$^{+/\Delta}$) and *Crif1* knockout (*Crif1*$^{-/\Delta}$) MEF cells using [U-^{13}C] glucose (n = 4, error bars indicate SD, *p < 0.05). Degree of ^{13}C-labeling in each metabolite can be estimated from relative intensity of higher *m/z* isotopomers with respect to non-labeled isotopomer, M0. Metabolic labeling was observed after cells were incubated with [U-^{13}C] glucose for 48 h. Closed and open circles represent ^{13}C and ^{12}C carbon, respectively, in each metabolite.

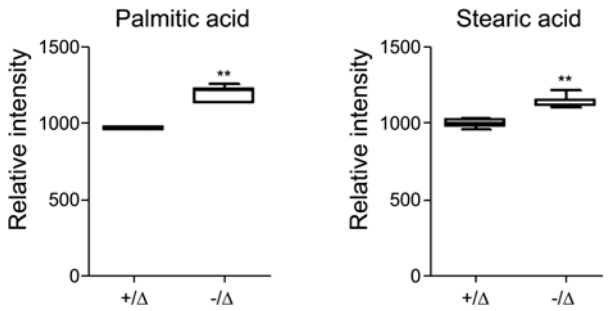

Figure 4. Relative abundances of fatty acids for normal (+/Δ) and *Crif1* knockout (–/Δ) MEF cells determined by GC-MS in the form of methyl esters after derivatization (n = 4, error bars indicate SD, **p < 0.01).

charge (Figure 2) which is calculated with the following equation;[22]

$$[ATP + 1/2(ADP)]/[(ATP) + (ADP) + (AMP)] \quad (1)$$

In *Crif1* deficiency, energy charge is lower mostly due to the loss of the major ATP source, OXPHOS subunits, and this could be one of the factors stimulating glucose uptake. Although *Crif1* deficient cells are consuming more glucose, respiratory oxidation through TCA cycle was suppressed remarkably and it was clearly demonstrated by the metabolic flux analysis using [U-^{13}C] glucose (Figure 4). It also showed that *Crif1* deficient cells are dependent more on anaerobic breakdown of pyruvate to form lactate, which is similar to the well-known Warburg effect in cancer cell metabolism.[11] The impairment of major OXPHOS complexes of mitochondria in *Crif1* deficiency induced noticeable changes in the metabolic profile of TCA cycle. In normal cells, significant fraction of the glycolysis metabolic flux enters into TCA cycle and contributes to the generation of ATPs and metabolic intermediates. *Crif1* knockout, by contrast, exhibited depletion of citrate pool in the cells indicating marked reduction of the metabolic flux from pyruvate into TCA cycle. The metabolic flux analysis using [U-^{13}C] glucose in Figure 3 also provided supporting evidence on the diminished metabolic flux from glycolysis into TCA cycle. M3 peak of lactate in Figure 3 indicates incorporation of three ^{13}C units originating from [U-^{13}C] glucose via pyruvate, while M2 peak of citrate in Figure 3 indicates incorporation of two ^{13}C units from pyruvate after 48 h of cell culture. Significant decrease of M2 peak as well as M3-M5 peaks of citrate from *Crif1* knockout cells clearly demonstrated suppressed metabolic flux into TCA cycle. Increased lactate level and predominance of fully ^{13}C-labeled lactate in *Crif1* knockout cells showed that the major glycolytic metabolic flux leaked into lactate, instead. It should be noted, however, the glycolytic metabolic flux into citrate was not suppressed completely in the mutant cells (see M2 peak for *Crif1* knockout cells).

Isotope (^{13}C) tracking for TCA cycle intermediates in the follow-up pathways, fumarate and malate, showed that the glycolytic metabolic flux was almost completely blocked in *Crif1* knockout cells. Both metabolites had negligible ^{13}C-labeling in the flux analysis using [U-^{13}C] glucose for 48 h. In spite of the blockage of metabolic flux, significant increases of fumarate and malate were observed in the static metabolite analysis as shown in Figure 2. Considering the conversion of isocitrate into 2-oxoglutarate catalyzed by isocitrate dehydrogenation is the rate-limiting step in the TCA cycle, the maintenance of TCA cycle operation observed here indicates alternative inputs potentially from amino acid catabolism. Several studies previously highlighted the utilization of amino acids in cancer cells as an alternative input of nutrients.[22,23] The same studies also demonstrated the existence of reverse (reductive) TCA cycle flux from 2-oxoglutarate to citrate, which is believed to be enhanced in hypoxia. Although the relative contributions of the TCA cycle in the forward (oxidative) or reverse (reductive) direction are not clear in the cells under investigation, present study implicates that the mitochondrial metabolism in *Crif1* deficient cells is mostly maintained by anaplerotic reactions of amino acids. It should be also noted that the maintenance of TCA cycle metabolism without utilization of NADH for OXPHOS reactions may result in accumulation of NADH in mitochondria. Increased NADH is known to suppress the conversion of isocitrate into 2-oxoglutarate by inhibiting isocitrate dehydrogenation activity. Indeed, significant de-

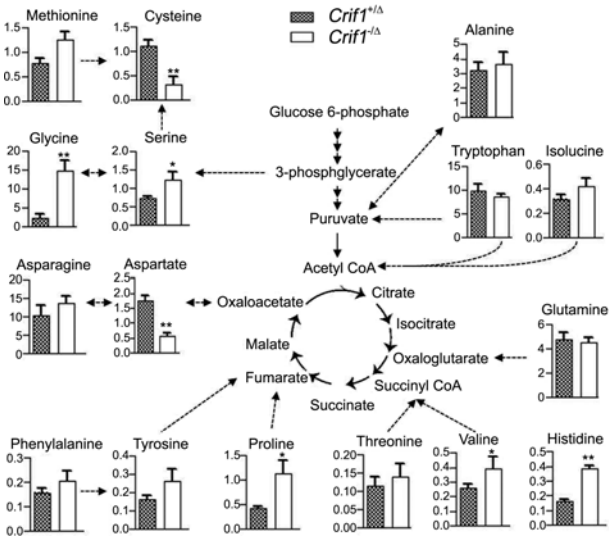

Figure 5. Relative abundances of amino acid metabolites for normal ($Crif1^{+/\Delta}$) and *Crif1* knockout ($Crif1^{-/\Delta}$) MEF cells (n = 4, error bars indicate SD, **p < 0.01, *p < 0.05).

crease of NAD/NADH ratio in *Crif1* deficient cells was observed (Figure 2).

Free fatty acids such as palmitic acid and stearic acid were increased noticeably in *Crif1* knockout cells (Figure 4). It could be due to increased synthesis of fatty acids from citrate exported to the cytosol. The lower level of citrate observed in *Crif1* knockout cells may be due to depletion of citrate pool for the lipid biosynthesis. Up-regulation of fatty acid biosynthesis is also well-known in most human carcinomas.[24,25]

To study the potential influence of ROS in *Crif1* deficiency metabolism, metabolic profile of *Crif1* knockout cells treated with NAC (–/Δ NAC), which is known as ROS scavenger, was also investigated. Mitochondrial ROS levels are known to increase significantly in *Crif1* deficiency[6] and may affect the glycolysis and TCA metabolism. However, treatment of NAC didn't show any difference in the metabolism of *Crif1* knockout cells as shown in Figure 2. It demonstrates that increased mitochondrial ROS doesn't have any direct impact on the *Crif1* deficiency metabolism and the altered metabolism of *Crif1* knockout cells is not due to excessive ROS.

Amino Acid Metabolism. To meet the need of metabolic reprogramming for adaptation to impaired OXPHOS function, changes in metabolic profile of amino acids is also expected. It's been also implicated in the metabolic profile of TCA cycle intermediates. Levels of most amino acids were significantly increased in *Crif1* knockout cells as shown in Figure 5 except for aspartate and cysteine. It should be noted that significant accumulation of all amino acids except for glutamine has been previously reported in tumors.[26] In the present cell culture experiments, changes in amino acids levels were not limited by the availability in the media, instead, more of the consequence of the balance between cellular uptake and metabolic consumption of amino acids. Hence, overall increase in levels of most amino acid observed in *Crif1* knockout cells is mostly probably the result of metabolic reprogramming to meet the needs of energy balance and anabolic precursors in mitochondria. More works are required to investigate the detailed mechanisms of metabolic adaptation including the unexpected decreases in aspartate and cysteine levels. Additional anaplerotic input (other than glutamine) into TCA cycle or other metabolic pathways may explain this observation. For example, carbon skeleton from aspartate was reported to metabolize through TCA cycle intermediates via oxaloacetate in astrocytes.[27]

Conclusion

In present study, the effect of *Crif1* deficiency with impaired OXPHOS function in cell metabolism was investigated for the first time using LC-MS/MS, high resolution LC-MS and GC-MS methods. *Crif1* knockout cells were characterized with high glucose uptake and lower oxygen consumption rate. Major glycolytic, TCA cycle and amino acid metabolites exhibited almost similar profiles with those of cancer cells. *Crif1* knockout cells consumed more glucose and produced significantly increased amounts of lactate in glycolysis, while the metabolic flux into TCA cycle was minimize. Levels of most amino acid were significantly increased in *Crif1* knockout cells mostly probably as a result of metabolic reprogramming to meet the needs of energy balance and anabolic precursors in mitochondria. Overall metabolic pattern of *Crif1* knockout MEF cells is quite similar to that of cancer cells in spite of different root of metabolic imbalance. Hence, we cannot rule out the possibility that different metabolic controls result in similar metabolic profiles due to excessive rebalancing for survival and proliferation.

Acknowledgments. This work was supported by the Korea Research Institute of Standards and Science (KRISS) under the project "Establishing Measurement Standards for Food and Environmental Analysis", grant 12011026, and "Development of Protein Measurement Standards", grant 12011021.

References

1. Chung, H. K.; Yi, Y. W.; Jung, N. C.; Kim, D.; Suh, J. M.; Kim, H.; Park, K. C.; Song, J. H.; Kim, D. W.; Hwang, E. S.; Yoon, S. H.; Bae, Y. S.; Kim, J. M.; Bae, I.; Shong, M. *J. Biol. Chem.* **2003**, *278*, 28079.
2. Suh, J. H.; Shong, M.; Choi, H. S.; Lee, K. *Mol. Endocrinol.* **2008**, *22*, 33.
3. Kwon, M. C.; Koo, B. K.; Moon, J. S.; Kim, Y. Y.; Park, K. C.; Kim, N. S.; Kwon, M. Y.; Kong, M. P.; Yoon, K. J.; Im, S. K.; Ghim, J.; Han, Y. M.; Jang, S. K.; Shong, M.; Kong, Y. Y. *EMBO J.* **2008**, *27*, 642.
4. Kwon, M. C.; Koo, B. K.; Kim, Y. Y.; Lee, S. H.; Kim, N. S.; Kim, J. H.; Kong, Y. Y. *J. Biol. Chem.* **2009**, *284*, 33634.
5. Kang, H. J.; Hong, Y. B.; Kim, H. J.; Bae, I. *J. Biol. Chem.* **2010**, *285*, 21258.
6. Kim, S. J.; Kwon, M.; Ryu, M. J.; Chung, H. K.; Tadi, S.; Kim, Y. K.; Kim, J. M.; Lee, S. H.; Park, J. H.; Kweon, G. R.; Ryu, S.-W; Jo, Y. S.; Lee, C.-H.; Hatakeyama, H.; Goto, Y.; Yim, Y.-H.; Chung, J.; Kong, Y.-Y.; Shong, M. *Cell Metab.* **2012**, *16*, 274.

7. Spratlin, J. L.; Serkova, N. J.; Eckhardt, S. G. *Clin. Cancer Res.* **2009**, *15*, 431.
8. Scalbert, A.; Brennan, L; Fiehn, O.; Hankemeier, T.; Kristal, B. S.; van Ommen, B.; Pujos-Guillot, E.; Verheij, E.; Wishart, D.; Wopereis, S. *Metabolomics* **2009**, *5*, 435.
9. Hirayama, A.; Kami, K.; Sugimoto, M.; Sugawara, M.; Toki, N.; Onozuka, H.; Kinoshita, T.; Saito, N.; Ochiai, A.; Tomita, M.; Esumi, H.; Soga, T. *Cancer Res.* **2009**, *69*, 4918.
10. Scott, D. A.; Richardson, A. D.; Filipp, F. V.; Knutzen, C. A.; Chiang, G. G.; Ronai, Z. e. A.; Osterman, A. L.; Smith, J. W. *J. Biol. Chem.* **2011**, *286*, 42626.
11. Warburg, O. *Science* **1956**, *123*, 309.
12. Kwon, M.-C.; Koo, B.-K.; Moon, J.-S.; Kim, Y.-Y.; Park, K. C.; Kim, N.-S.; Kwon, M. Y.; Kong, M.-P.; Yoon, K.-J.; Im, S.-K.; Ghim, J.; Han, Y.-M.; Jang, S. K.; Shong, M.; Kong, Y.-Y. *Embo J.* **2008**, *27*, 4.
13. Wu, J. J.; Quijano, C.; Chen, E.; Liu, H.; Cao, L.; Fergusson, M. M.; Rovira, I. I.; Gutkind, S.; Daniels, M. P.; Komatsu, M.; Finkel, T. *Aging* **2009**, *1*, 425.
14. Ni, Q.; Reid, K. R.; Burant, C. F.; Kennedy, R. T. *Anal. Chem.* **2008**, *80*, 3539.
15. Luo, B.; Groenke, K.; Takors, R.; Wandrey, C.; Oldiges, M. *J. Chromatogr. A* **200**7, *1147*, 153.
16. Ichihara, K. I.; Fukubayashi, Y. *J. Lipid Res.* **2010**, *51*, 635.
17. Joo, H. J.; Yim, Y.-H.; Jeong, P. Y.; Jin, Y.; Lee, J. E.; Kim, H.; Jeong, S. K.; Chitwood, D. J.; Paik, Y. K. *Biochem. J.* **2009**, *422*, 61.
18. Ahn, W. S.; Antoniewicz, M. R. *Metab. Engineer.* **2011**, *13*, 508.
19. Roberts, L. D.; Murray, A. J.; Menassa, D.; Ashmore, T.; Nicholls, A. W.; Griffin, J. L. *Genome Biol*. **2011**, *12*, R75.
20. Harder, U.; Boletzko, B.; Peissner, W. *J. Chromatogr. B* **2011**, *879*, 495.
21. Norberg, K.; Siesjo, B. K. *Brain Res.* **1975**, *86*, 31.
22. Chapman, A. G.; Fall, L.; Atkinson, D. E. *J. Bacteriol.* **1971**, *108*, 1072.
23. Dillona, E. L.; Volpia, E.; Wolfeb, R. R.; Sinhaa, S.; Sanfordb, A. P.; Arrastiac, C. D.; Urbana, R. J.; Caspersona, S. L.; Paddon-Jonesa, D.; Sheffield-Moorea, M. *Clin. Nutr.* **2007**, *26*, 736.
24. Yang, C.; Richardson, A. D.; Smith, J. W.; Osterman, A. *Pacific Symposium on Biocomputing* **2007**, *12*, 181.
25. Kuhajda, F. P. *Cancer Res.* **2006**, *66*, 5977.
26. Metallo, C. M.; Gameiro, P. A.; Bell, E. L.; Mattaini, K. R.; Yang, J.; Hiller, K.; Jewell, C. M.; Johnson, Z. R.; Irvine, D. J.; Guarente, L.; Kelleher, J. K.; van der Heiden, M. G.; Iliopoulos, O.; Stephanopoulos, G. *Nature* **2011**, *20*, 481.
27. Bakken, I. J.; White, L. R.; Aasly, J.; Unsgård, G.; Sonnewald, U *Glia* **1998**, *23*, 271.